

# **Validation of a Computed Tomography (CT) based Fractional Flow Reserve (FFR) software using the 320 Detectors Aquilion ONE CT Scanner**

NCT03149042

September 24, 2019

## **Research Team**

Dr. Ciprian N Ionita (Principal Investigator)

Kelsey Sommer BS (Study Coordinator / Investigator)

Dr. Erin Angel (Investigator)

Dr. Vijay Iyer (Investigator)

Dr. Kanako Kunishima Kumamaru (Investigator)

Dr. Dimitris Mitsouras (Investigator)

Dr. Frank Rybicki (Investigator)

Dr. Michael F Wilson (Investigator)

## **Contents**

Glossary.....	3
Background and Rationale.....	4
Summary of Proposed Research.....	5
Objectives.....	6
Hypothesis.....	6
Study Design / Procedures.....	7-8
Inclusion Criteria.....	9
Exclusion Criteria.....	9
Sample size.....	9
Study Flow Chart.....	10
Statistical Analysis.....	10
References.....	11-13

## **Glossary**

FFR = Fractional Flow Reserve

CCTA = Coronary Computed Tomography Angiography

I-FFR = Invasive Fractional Flow Reserve

CT-FFR = Computed Tomography Fractional Flow Reserve

B-FFR = Benchtop Fractional Flow Reserve

ROC = Receiver Operating Characteristic

AUC = Area Under the Curve

STL= Stereo Lithographic

## **Background and Rationale**

In the last few years there has been a significant push to develop and implement coronary blood flow estimation based on computed tomography angiography. Clinical trials such as FAME (Fractional Flow Reserve versus Angiography for Multivessel Evaluation) and FAME II demonstrated: “added benefit of physiologic information, specifically fractional flow reserve (FFR), above anatomic information alone, in guiding intervention in patients with multivessel coronary disease undergoing intervention and patients with stable coronary disease. Anatomic information with physiologic information obtained via FFR-CT, can help identify patients who would or would not benefit from revascularization.

The results of these studies were very promising, however, some of these approaches failed to meet the required accuracy or required changes in acquisition protocols which increased the dose delivered to the patient. For example the 17-center DeFACTO (Determination of Fractional Flow Reserve by Anatomic Computed Tomographic Angiography) study, showed that FFR-CT can improve diagnostic accuracy and discrimination versus CTA alone but failed to meet its pre-specified primary outcome goal for the level of per-patient diagnostic accuracy. We believe that these inaccuracies are a direct consequence of the arbitrary boundary conditions imposed in order to solve the Navier –Stokes equations and optimization of acquisition parameters.

The main aim of this proposal is aligned with the studies above. We propose to improve the FFR-CT accuracy using the new opportunities offered by 3D printing. Namely we will develop very accurate coronary models using 3D printing and use these phantoms to optimize the FFR-CT approach. Next we propose to use the optimized approach to perform a small clinical study at Gates Vascular Institute where we will correlate the FFR-CT results with angio FFR and patient follow-up.

## Summary of Proposed Research

Coronary Computed Tomography Angiography (CCTA) contrast opacification gradients and FFR-CT estimation can aid in the severity estimation of significant atherosclerotic lesions. Following this trend, we recently developed a collaboration between Brigham and Women's Hospital (BWH) and Gates Vascular Institute (GVI). We 3D-printed patient specific coronary phantoms at (GVI) and scanned them with a Toshiba Aquilion scanner to test several aspects of the contrast opacification gradients using a method established at BWH. Our initial results showed strong correlation between the flow in the phantom and opacification gradients. We believe that this approach could be further developed to test and validate FFR-CT algorithms. Currently, FFR-CT algorithms can only be optimized using theoretical models and can only be validated in large multi-center clinical trials. This phantom approach would allow optimization of FFR-CT algorithms with a measured validation technique without the need for large clinical trials. Thus we believe that this study will result in a FFR-CT algorithm/method with a better predictability for arterial lesion severity than those existing on the market today. Our approach is to use the infrastructure at GVI to perform a detailed validation of the FFR-CT method using 3D printed patient specific phantoms. Each patient will have a 3D phantom printed, containing the culprit lesion and used in a benchtop flow analysis. Flow measurements will be compared with: CT-FFR for both patients and phantoms, angio lab FFR measurements and 30 days follow-up. This pilot clinical study will include ~50 patients over a year and half at GVI. We are confident that this approach performed via 3D-phantom testing will prove the validity of FFR-CT based measurements as well as develop a new standard for validating FFR-CT algorithms

## Objectives

- To build 50 3D printed patient specific phantoms for benchtop testing to determine pressure gradient along diseased vasculature
- To perform a detailed validation of the FFR-CT method using 3D printed patient specific phantoms
- Optimization of FFR-CT algorithms with a better predictability for arterial lesion severity without the need for large clinical trials

## Hypotheses

Flow simulations in 3D printed patient specific phantoms will correlate with CT derived fractional flow reserve calculations. To demonstrate the concept feasibility, we propose to use 3D printed cardiac models for software validation using clinical evaluation as a gold standard. The clinical cases will be used both as ground truth to demonstrate the accuracy of the phantom validation as well as a pilot single-center clinical evaluation to demonstrate similar results to previously published clinical trials for algorithms similar to those being tested.

## Study Design/ Procedures

Patients will be consented after CCTA. First requirement is that the patient has at least one lesion with >50% stenosis or 30-50% if clinically driven. Second requirement is that the patient undergoes a cath lab intervention. If one of the above requirements is not satisfied the patient will be removed from the study. Viable candidates based on inclusion/exclusion criteria will undergo clinically indicated first generation 320-detector row CCTA (Aquilion ONE, Canon Medical Systems, Tustin, CA) with 0.5 mm slice thickness, automated tube current modulation, 100 kVp, and a reconstructed voxel size of 0.625x0.625x0.5 mm. Next, the patient will undergo catheter lab procedure as clinically warranted. The invasive FFR will be done on the culprit lesion(s) for clinical purposes. Invasive FFR (I-FFR) will be recorded via pressure wire at a distance of two lesion lengths past the distal end of the lesion. A FFR cutoff value of less than or equal to 0.8 was used to determine hemodynamic significance.

For each patient a 3D printed phantom will be made and tested. Segmentation will be performed in Vitrea, vascular mesh sculpting in Autodesk Meshmixer, and 3D printed in a Stratasys Eden 260V printer (Stratasys, Eden Prairie, MN) printer. Figure 1 shows the model development process. Each 3D printed patient-specific model will be connected to a flow loop using the CardioFlow 5000 MR programmable physiological pulsatile flow pump (Shelley Medical Imaging Technologies, Toronto, Ontario, Canada) and a Benchtop FFR will be obtained. This pump introduced a physiologic human cardiac waveform and provided also an ECG signal triggered at points within the cardiac waveform. The viscosity of blood (approximately 3.7 cP) will be mimicked using a glycerol water solution of 40% water and 60% glycerol and measured using a viscometer. Figure 2 shows the benchtop flow system.

Reconstructed CCTA images were imported into Vitrea segmentation software (Vital Images, Minnetonka, MN) using the research-based CT-FFR algorithm [26-28]. The software analyzes four data volumes acquired a 70-99% of the R-R interval and computes the FFR based on the changes in vessel diameter and computational fluid dynamics.

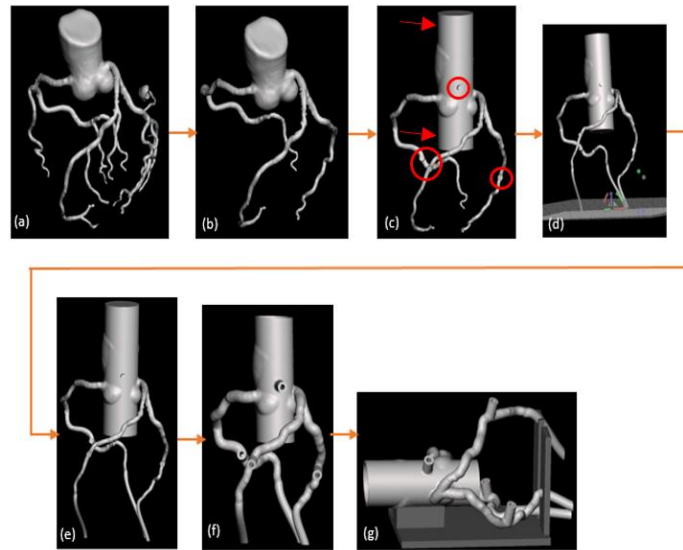


Figure 1: Model development process. (a) The cardiac mesh was exported as a stereolithographic file from Vitrea into Autodesk Meshmixer. (b) The daughter branches off of the 3 main coronary arteries were cut off from the mesh. (c) The aortic root was extended at both the outlet and inlet with 30 mm diameter for later connections (red arrows). Cylindrical meshes were appended (red circles) to the aortic root and each of the coronary arteries for later pressure sensor connections. (d) Each coronary artery was extended. (e) A plane cut was administered at the vessel outlets for parallel ends. (f) A 2 mm wall was generated while preserving the geometry of the arteries. (g) A support structure is positioned around the model and the Boolean union operation is administered.

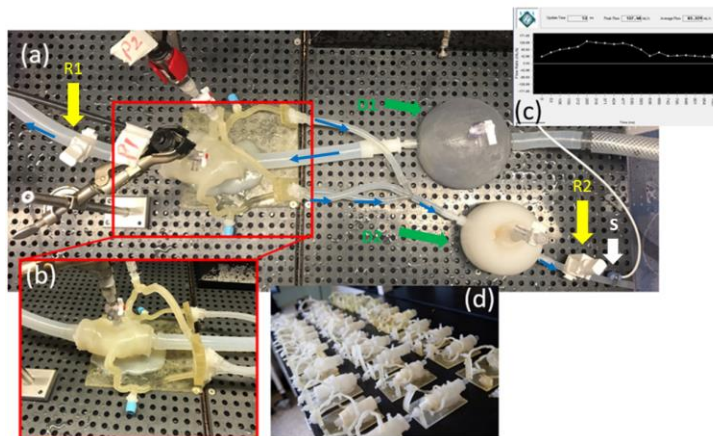


Figure 2: Benchtop flow system. (a) A 3D printed patient-specific coronary model is connected to a flow loop using the Cardio Flow 5000 MR programmable physiological pulsatile flow pump (Shelley Medical Imaging Technologies, Toronto, Ontario, Canada). The flow loop consisted of two compliance chambers, at the aortic inlet (D1) and distal to the coronary arteries (D2) to control pressure oscillation and distal resistance. Aortic base pressure and distal flow rate were controlled by adjustable mechanical clamps (R1 and R2 respectively), and flow rate was recorded using an ultrasonic flow sensor (S). Flow direction is indicated by blue arrows. (b) Detailed side view of the 3D printed coronary model with pressure sensors connected to the aorta and the LAD. (c) Coronary waveform within the coronary flow pump software to determine the flow rate (mL/s) as a function of time in a single cardiac cycle. (d) 52 patient-specific 3D printed coronary models assembled and ready to go through flow testing.

## Inclusion Criteria

- Scheduled for clinically mandated elective invasive coronary angiography (ICA) or clinically mandated CTA
- >18 yrs of age

## Exclusion Criteria

- Less than 30 years of age
- Atrial fibrillation
- Renal insufficiency (estimated glomerular filtration rate (GFR) <60 ml/min/1.73 m<sup>2</sup>)
- Active Bronchospasm prohibiting the use of beta blockers
- Morbid obesity (body mass index 40 kg/m<sup>2</sup>)
- Contraindications to iodinated contrast
- Emergencies requiring immediate intervention or patients unable to consent
- Patients not showing coronary calcium during Calcium Scoring procedures

## Sample Size

To determine the numbers of phantoms needed for this study we treated 3D printing as a new diagnostic tool for which we needed to assess the accuracy of detecting significant FFR values. We used the sample size calculation proposed by Flahault et. al. [23].

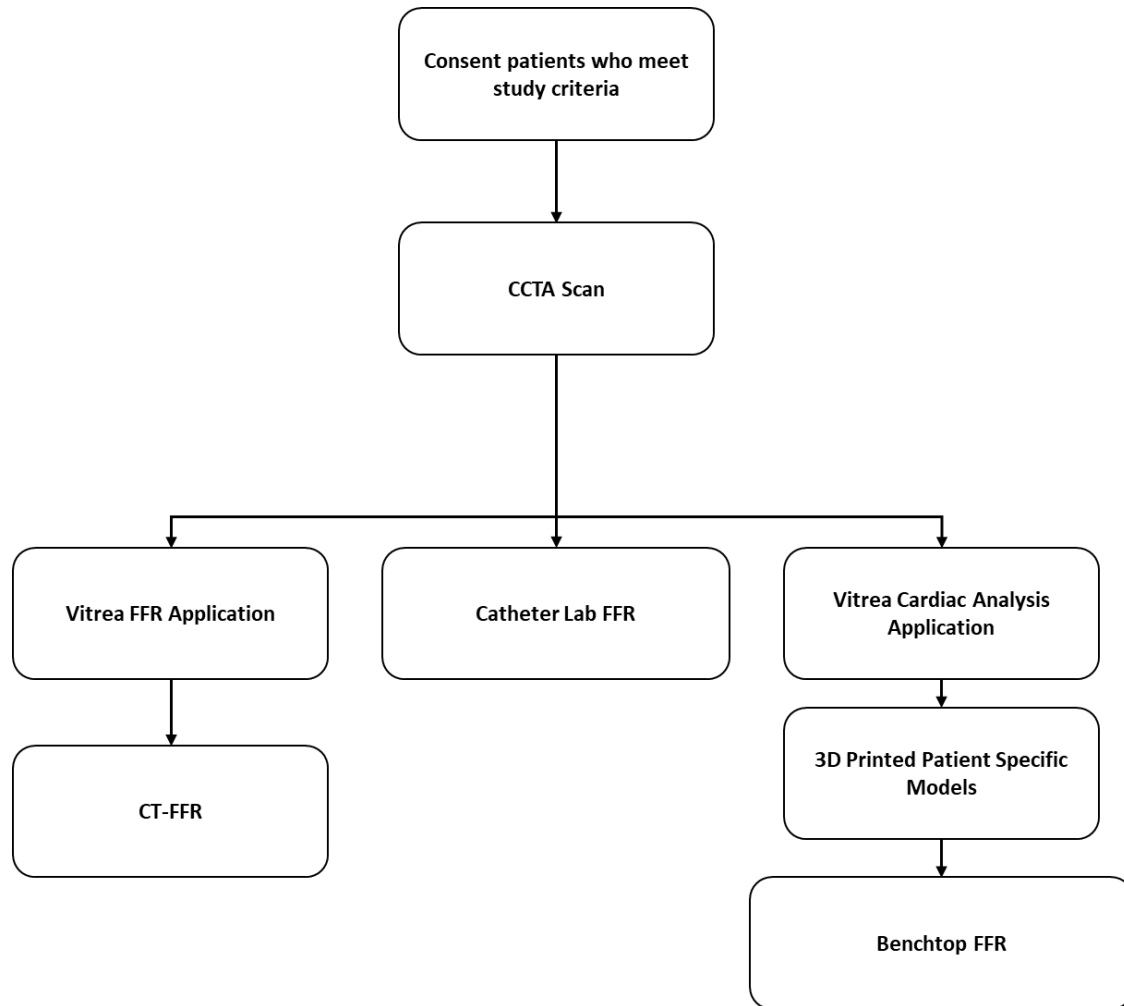
$$n = \frac{\left( z_{\alpha/2} \sqrt{\hat{V}(\hat{A})} \right)^2}{L^2}$$

Since this is a technical feasibility study, we wanted to estimate the ROC area to within  $\pm 0.06$ ; thus,  $L=0.12$  and the confidence level was set at 0.92 which corresponds to  $z_{(\alpha/2)}=1.75$ . For the variance function we used the formulation indicated by Obuchowski et al. [24] who proposed an estimate of the variance function for the Receiver Operator Characteristic based on an exponential distribution.

$$\hat{V}(\hat{A}) = (0.0099 \times e^{a^2/2}) \times [(5a^2 + 8) + (5a^2 + 8)/R]$$

R denotes the ratio of the number of patients without the condition to patients with the condition in the study sample. Using results from previous reports on CT-FFR [25], we set  $R=1.2$ . For an AUROC=0.8 the parameter may be set to 1.19 [24]. Thus the number of samples with  $FFR \leq 0.80$  are approximately 23 and the total number of subject given by  $N_{total}=n(1+R)$  is approximately 52.

## Study Flow Chart



## Statistical Analysis

The absolute error as a percentage with 95% confidence intervals and Pearson correlation values will be calculated to assess the results obtained from the benchtop flow testing and the CT-FFR software and how they compared to the I-FFR reference standard. A ROC curve will also be generated to determine the area under the curve (AUC) for B-FFR and CT-FFR when compared to I-FFR. Statistical analysis for the development of the ROC curves and correlation analysis will be completed within NCSS Statistical Software (NCSS, v.12, LLC, Kaysville, Utah).

## References

1. Brown, B.G., et al., Quantitative coronary arteriography: estimation of dimensions, hemodynamic resistance, and atheroma mass of coronary artery lesions using the arteriogram and digital computation. *Circulation*, 1977. 55(2): p. 329-337.
2. Qureshi, A.I., et al., Prevention and treatment of thromboembolic and ischemic complications associated with endovascular procedures: Part I— Pathophysiological and pharmacological features. *Neurosurgery*, 2000. 46(6): p. 1344-1359.
3. Kumamaru, K.K., et al., Diagnostic accuracy of 3D deep-learning-based fully automated estimation of patient-level minimum fractional flow reserve from coronary computed tomography angiography. *European Heart Journal - Cardiovascular Imaging*, 2019.
4. Tang, C.X., et al., Diagnostic performance of fractional flow reserve derived from coronary CT angiography for detection of lesion-specific ischemia: A multi-center study and meta-analysis. *Eur J Radiol*, 2019. 116: p. 90-97.
5. Morris, P.D., et al., Virtual fractional flow reserve from coronary angiography: modeling the significance of coronary lesions: results from the VIRTU-1 (VIRTUal Fractional Flow Reserve From Coronary Angiography) study. *JACC Cardiovasc Interv*, 2013. 6(2): p. 149-57.
6. Morris, P.D., et al., Computational fluid dynamics modelling in cardiovascular medicine. *Heart*, 2016. 102(1): p. 18-28.
7. Sankaran, S., et al., Uncertainty quantification in coronary blood flow simulations: Impact of geometry, boundary conditions and blood viscosity. *J Biomech*, 2016. 49(12): p. 2540-7.
8. Sankaran, S., et al., Uncertainty quantification in coronary blood flow simulations: impact of geometry, boundary conditions and blood viscosity. *Journal of biomechanics*, 2016. 49(12): p. 2540-2547.
9. Ko, B.S., et al., Noninvasive CT-derived FFR based on structural and fluid analysis: a comparison with invasive FFR for detection of functionally significant stenosis. *JACC: Cardiovascular Imaging*, 2017. 10(6): p. 663-673.
10. Modi, B.N., et al., Optimal Application of Fractional Flow Reserve to Assess Serial Coronary Artery Disease: A 3D-Printed Experimental Study With Clinical Validation. *J Am Heart Assoc*, 2018. 7(20): p. e010279.
11. Shepard, L.M., et al., Initial evaluation of three-dimensionally printed patient-specific coronary phantoms for CT-FFR software validation. *J Med Imaging (Bellingham)*, 2019. 6(2): p. 021603.

12. Sommer, K.N., et al. 3D printed cardiovascular patient specific phantoms used for clinical validation of a CT-derived FFR diagnostic software. in SPIE Medical Imaging. 2018. SPIE.
13. Shepard, L., et al. Initial simulated FFR investigation using flow measurements in patient-specific 3D printed coronary phantoms. in Medical Imaging 2017: Imaging Informatics for Healthcare, Research, and Applications. 2017. International Society for Optics and Photonics.
14. Rengier, F., et al., 3D printing based on imaging data: review of medical applications. International journal of computer assisted radiology and surgery, 2010. 5(4): p. 335-341.
15. Son, K.H., et al., Surgical planning by 3D printing for primary cardiac schwannoma resection. Yonsei medical journal, 2015. 56(6): p. 1735-1737.
16. Chepelev, L., et al., Radiological Society of North America (RSNA) 3D printing Special Interest Group (SIG): guidelines for medical 3D printing and appropriateness for clinical scenarios. 3D printing in medicine, 2018. 4(1): p. 11.
17. Kim, H.J., et al., Patient-specific modeling of blood flow and pressure in human coronary arteries. Ann Biomed Eng, 2010. 38(10): p. 3195-209.
18. O'Rourke, M.F., et al., Clinical applications of arterial stiffness; definitions and reference values. American journal of hypertension, 2002. 15(5): p. 426-444.
19. Rutishauser, W., Towards measurement of coronary blood flow in patients and its alteration by interventions. European heart journal, 1999. 20(15): p. 1076-1083.
20. Tabaczynski, J., Mechanical Assessment of 3D Printed Patient Specific Phantoms for Simulation of Minimally Invasive Image Guided Procedures. 2018, State University of New York at Buffalo.
21. Tabaczynski, J.R., et al. Use of patient specific 3D printed (3DP) neurovascular phantoms for mechanical assessment of devices used in image guided minimally invasive procedures. in Medical Imaging 2018: Imaging Informatics for Healthcare, Research, and Applications. 2018. International Society for Optics and Photonics.
22. Sommer, K., et al. Design optimization for accurate flow simulations in 3D printed vascular phantoms derived from computed tomography angiography. in Medical Imaging 2017: Imaging Informatics for Healthcare, Research, and Applications. 2017. International Society for Optics and Photonics.
23. Fahraeus, R. and T. Lindqvist, The viscosity of the blood in narrow capillary tubes. American Journal of Physiology-Legacy Content, 1931. 96(3): p. 562-568.
24. Williams, B., et al., Differential impact of blood pressure-lowering drugs on central aortic pressure and clinical outcomes: principal results of the Conduit

Artery Function Evaluation (CAFE) study. *Circulation*, 2006. 113(9): p. 1213-1225.

25. Kanaji, Y., et al., Effect of elective percutaneous coronary intervention on hyperemic absolute coronary blood flow volume and microvascular resistance. *Circulation: Cardiovascular Interventions*, 2017. 10(10): p. e005073.
26. Ko, B., et al., Novel non-invasive CT-derived fractional flow reserve based on structural and fluid analysis (CT-FFR) for detection of functionally significant stenosis: a comparison with invasive fractional flow reserve. *JACC Cardiovasc Imaging*, 2017. 10: p. 663-73.
27. Ihdahid, A.R., et al., Performance of computed tomography-derived fractional flow reserve using reduced-order modelling and static computed tomography stress myocardial perfusion imaging for detection of haemodynamically significant coronary stenosis. *European Heart Journal-Cardiovascular Imaging*, 2018. 19(11): p. 1234-1243.
28. Fujimoto, S., et al., Diagnostic performance of on-site computed CT-fractional flow reserve based on fluid structure interactions: comparison with invasive fractional flow reserve and instantaneous wave-free ratio. *European Heart Journal - Cardiovascular Imaging*, 2018. 20(3): p. 343-352.
29. Kishi, S., et al., Fractional flow reserve estimated at coronary CT angiography in intermediate lesions: comparison of diagnostic accuracy of different methods to determine coronary flow distribution. *Radiology*, 2017. 287(1): p. 76-84.
30. Li, P., et al., Blooming Artifact Reduction in Coronary Artery Calcification by A New De-blooming Algorithm: Initial Study. *Scientific reports*, 2018. 8(1): p. 6945.
31. Romano, S.M. and M. Pistolesi, Assessment of cardiac output from systemic arterial pressure in humans. *Critical care medicine*, 2002. 30(8): p. 1834-1841.
32. Cotter, G., et al., The role of cardiac power and systemic vascular resistance in the pathophysiology and diagnosis of patients with acute congestive heart failure. *European journal of heart failure*, 2003. 5(4): p. 443-451.
33. Moore, T.J., et al., Estimated costs of pivotal trials for novel therapeutic agents approved by the US Food and Drug Administration, 2015-2016. *JAMA internal medicine*, 2018. 178(11): p. 1451-1457.